# Entanglement generation between Unruh-DeWitt detectors in the de Sitter spacetime – analysis with complex scalar fields

Shagun Kaushal $^{1,2,*}$  and Sourav Bhattacharya $^{3,\dagger}$ 

<sup>1</sup>Department of Physics, Vellore Institute of Technology, Vellore, Tamil Nadu 632 014, India<sup>c</sup>

<sup>2</sup>Department of Physics, Indian Institute of Technology Delhi, Hauz Khas, New Delhi 110 016, India

<sup>3</sup>Relativity and Cosmology Research Centre, Department of Physics,

Jadavpur University, Kolkata 700 032, India

We investigate the entanglement generation or harvesting between two identical, comoving Unruh-DeWitt detectors in the cosmological de Sitter spacetime. The detectors are assumed to be unentangled initially. They are individually coupled to a complex scalar field, which eventually leads to coupling between themselves. Two kinds of complex scalar fields are investigated here — conformally invariant and massless minimally coupled. By tracing out the degrees of freedom corresponding to the scalar, we construct the reduced density matrix for the two detectors, whose eigenvalues characterise transition probabilities between the energy levels of the detectors. We have computed the negativity, quantifying the degree of entanglement generated at late times between the two detectors. The similarities and differences of these results between the aforementioned two kinds of scalar fields have been discussed. We also compare our results with the existing result of the real scalar field, and point out the qualitative differences. In particular, we emphasise that entanglement harvesting is more resilient in scenarios involving complex fields and nonlinear couplings.

<sup>&</sup>lt;sup>c</sup> Current affiliation

<sup>\*</sup> shagun.kaushal@vit.ac.in, shagun123@iitd.ac.in

<sup>†</sup> sbhatta.physics@jadavpuruniversity.in

#### **CONTENTS**

1.	Introduction	2
II.	The basic setup	4
	A. Complex scalar field coupled to two Unruh-DeWitt detectors	7
III.	Computation of the transition integrals and the negativity	10
	A. A complex conformal scalar field	10
	B. The massless minimally coupled scalar field	12
IV.	Conclusion	14
A.	A brief sketch of the computation of Eq. (39) and Eq. (40)	16
В.	Asymptotic analysis of integrals Eq. (37), Eq. (38), Eq. (44) and Eq. (45)	18
	References	22

#### I. INTRODUCTION

The phenomenon of quantum entanglement, owing to its non-local characteristics, is considered to be even more counter intuitive compared to the standard quantum mechanical processes. Experimental observations, for example, of the violation of the Bell inequalities, which cannot be explained by classical theories based on hidden variables, have placed quantum entanglement on very strong physical grounds [1–4]. One of the defining characteristics of entangled states is the inability to describe the corresponding Hilbert space as a product of pure states of subsystems, e.g. [5, 6] and references therein. In addition to its foundational role in quantum physics, quantum entanglement has already found a wide range of applications in e.g., building high security communication systems by employing quantum cryptography to futuristic quantum teleportation-based devices, e.g. [7–11].

Recently, the research community has shown considerable interest in studying quantum entanglement in the context of relativistic quantum field theory [12–23]. An essential focus of this topic is to examine the dynamics of particles coupled to a quantum field, particularly using particle detectors. These investigations encompass studying entanglement dynamics, entanglement harvesting, and understanding the radiative processes of entangled relativistic particles [24–33].

Entanglement harvesting in particular, can be highly exciting, for it can offer means to extract additional quantum information.

The Unruh-DeWitt detectors are very popular in the context of relativistic quantum entanglement. Initially designed for studying radiation observed by a uniformly accelerated observer in the Minkowski spacetime, they were also used for studying Hawking radiation in eternal black hole spacetimes [34] (see also [35] and references therein). In this paper, we wish to examine the conditions under which these detectors become entangled over time in the presence of a coupling with a quantum field; such a framework allows us to explore the potential for entanglement harvesting between initially uncorrelated detectors. Various earlier investigations show different factors could contribute to this detector entanglement, including detectors' trajectories [12, 36–40], the background spacetime geometry [11, 41–50], the presence of a thermal bath [51–53], and even the transient passage of gravitational waves [54–58].

A large number of works have actively engaged in understanding the entanglement harvesting patterns of Unruh-DeWitt detectors that interact perturbatively with quantum fields. These works span from inertial detectors in flat spacetime [30, 38, 39, 52] to those following various trajectories in curved spacetimes [11, 13, 14, 41, 59–61]. For various such studies, we further refer our reader to [12, 36, 37, 40, 51, 53, 55, 62, 63] (also references therein). See [64, 65] for study of degradation/entanglement generation between two initially correlated Unruh-DeWitt detectors. See also [66, 67] for discussion on some non-perturbative effects. We note that studying such features of entanglement in the early inflationary background can provide valuable insights about the geometry as well as the quantum condition at such stage. For instance, entanglement generated in the early universe could affect cosmological correlation functions or the cosmic microwave background [68–70]. Researchers are increasingly interested in investigating aspects of entanglement in the cosmological de Sitter spacetime, for more details, readers may refer to [71–81].

In this work, we focus on examining entanglement harvesting between two two-level, identical, initially unentangled Unruh-DeWitt detectors coupled to a complex scalar field in the cosmological de Sitter spacetime. Note that for the complex scalar, the hermiticity of the field-detector coupling makes it qualitatively different from the real scalar. We take the trajectories of these detectors to be comoving, i.e., their spatial positions are fixed. However, their proper separation will increase with time due to the spacetime expansion. We investigate two physically interesting scenarios: a conformal complex scalar in the conformal vacuum and a minimally coupled complex massless scalar. We assume that the detectors are initially at ground state, whereas the initial state of the field is the vacuum. By constructing the appropriate reduced density matrix for the detectors at

the leading perturbative order, we next compute the logarithmic negativity for each scenario to quantify the entanglement generated or harvested between the detectors. Furthermore, we explore how the characteristics of this harvested entanglement vary with different system parameters, including their spatial separation. Single Unruh-DeWitt detector response functions for the above kinds of scalars in the de Sitter background can be seen in [79, 81].

The rest of this paper is organised as follows. In the next section, we briefly review the basic framework. Section III focuses on the entanglement generation or harvesting for detectors coupled to complex conformal and massless minimal scalar fields, by computing the negativity. Finally, we conclude in Section IV. Appendix A and Appendix B provide additional details of our calculations, following and in some instance extending the method outlined in [57] for a real scalar field theory. We will work with the mostly positive signature of the metric and will set  $c = 1 = \hbar$  throughout.

#### II. THE BASIC SETUP

Following [34, 35, 79–82], we wish to sketch below the basic setup we will be working in, for the sake of completeness. The de Sitter metric in expanding cosmological coordinates reads

$$ds^{2} = -d\tau^{2} + e^{2H\tau} \left( dx^{2} + dy^{2} + dz^{2} \right) = \frac{1}{H^{2}\eta^{2}} \left[ -d\eta^{2} + dx^{2} + dy^{2} + dz^{2} \right]$$
(1)

where H > 0 is the de Sitter Hubble constant, and  $\eta = -e^{-H\tau}/H$ , is the conformal time.

The general action for a complex scalar field reads

$$S = -\frac{1}{2} \int \sqrt{-g} \, d^4x \, \left[ (\nabla_{\mu} \phi^{\dagger}) (\nabla^{\mu} \phi) + (m^2 + \xi R) |\phi|^2 \right]$$
 (2)

We will be concerned with two scenarios in this paper, viz., a conformally invariant complex scalar field  $(m^2 = 0, \xi = 1/6)$  and a massless minimally coupled complex scalar  $(m^2 = 0 = \xi)$ .

Let us now quickly review the Unruh-DeWitt particle detector formalism, e.g. [34, 35]. For a real scalar field, the simplest coupling with a point-like detector reads

$$\mathcal{L}_{\text{int,real}} = -g\mu(\tau)\phi(x(\tau)) \tag{3}$$

where  $\mu$  is detector's monopole moment operator, g is the field-detector coupling constant, and  $\tau$  is the cosmological time along the trajectory of the detector. In the Heisenberg picture, we have  $\mu(\tau) = e^{iH_0\tau} \mu e^{-iH_0\tau}$ , where  $H_0$  is detector's free Hamiltonian. In this paper, we wish to restrict ourselves to comoving trajectories, i.e., we assume that the spatial position of the detector is fixed. However, their physical separation will change due to spacetime expansion.

For a transition from an initial state to a final state  $|i\rangle \rightarrow |f\rangle$  in this system, the first-order transition matrix element reads

$$\mathcal{M}_{fi} = ig \langle \omega_f | \mu | \omega_i \rangle \int_{\tau_i}^{\tau_f} d\tau e^{-i(\omega_f - \omega_i)\tau} \langle \phi_f | \phi(x(\tau)) | \phi_i \rangle$$
 (4)

where we have taken  $|i\rangle = |\omega_i\rangle \otimes |\phi_i\rangle$  and  $|f\rangle = |\omega_f\rangle \otimes |\phi_f\rangle$ , where  $\omega$ 's are the energy eigenvalues of the detector. The transition probability is given by

$$|\mathcal{M}_{fi}|^2 = g^2 |\langle \omega_f | \mu | \omega_i \rangle|^2 \int_{\tau_i}^{\tau_f} d\tau_1 d\tau_2 e^{-i(\omega_f - \omega_i)(\tau_1 - \tau_2)} \langle \phi_i | \phi(x_2(\tau_2)) | \phi_f \rangle \langle \phi_f | \phi(x_1(\tau_1)) | \phi_i \rangle$$
 (5)

We next sum over all the final states of the field, using the completeness relation for the field basis,  $|\phi_f\rangle$ . Assuming the initial state for the field to be the vacuum, we have the transition probability

$$\overline{\mathcal{F}}(\Delta\omega) = \int \mathcal{D}\phi_f |\mathcal{M}_{fi}|^2 = g^2 |\langle \omega_f | \mu | \omega_i \rangle|^2 \int_{\tau_i}^{\tau_f} d\tau_1 d\tau_2 e^{-i(\omega_f - \omega_i)(\tau_1 - \tau_2)} \langle \phi_i | \phi(x_2(\tau_2)) \phi(x_1(\tau_1)) | \phi_i \rangle$$
(6)

where

$$\langle \phi_i | \phi(x_2(\tau_2)) \phi(x_1(\tau_1)) | \phi_i \rangle \equiv iG^+(x_2(\tau_2) - x_1(\tau_1))$$

is the Wightman function. One then defines two new temporal variables

$$\Delta \tau = \tau_1 - \tau_2 \quad \text{and} \quad \tau_+ = \frac{\tau_1 + \tau_2}{2} \tag{7}$$

with ranges  $-\infty < \Delta \tau < \infty$ ,  $-\infty < \tau_+ < \infty$ . However, since the Wightman function usually is not a function of  $\tau_+$ , Eq. (6) is divergent. In order to thus give it a physical meaning, one defines transition probability per unit proper time by dividing/differentiating it by  $\tau_+$  [34]. The resulting transition probability per unit proper time is known as the response function, given by

$$\frac{d\mathcal{F}(\Delta\omega)}{d\tau_{+}} = \int_{-\infty}^{\infty} d\Delta\tau \, e^{-2i(\omega_{f} - \omega_{i})\Delta\tau} \, iG^{+}(\Delta\tau) \tag{8}$$

where we have abbreviated  $\mathcal{F} := \overline{\mathcal{F}}/(g|\langle \omega_f | \mu | \omega_i \rangle|)^2$ .

For a scalar field moving in Eq. (1) of mass m and non-minimal coupling  $\xi$ , the Wightman function  $iG^+(x,x')$  reads [82],

$$iG^{+}(x,x') = \frac{H^{2}}{16\pi^{2}}\Gamma\left(\frac{3}{2} - \nu\right)\Gamma\left(\frac{3}{2} + \nu\right) {}_{2}F_{1}\left(\frac{3}{2} - \nu, \frac{3}{2} + \nu, 2; 1 - \frac{y(x,x')}{4}\right)$$
(9)

where

$$\nu = \left(\frac{9}{4} - 12\xi - \frac{m^2}{H^2}\right)^{1/2}$$

and the de Sitter invariant interval y(x, x') reads

$$y(x, x') = \frac{-(\eta - \eta' - i\epsilon)^2 + |\vec{x} - \vec{x}'|^2}{\eta \eta'}$$

where  $\epsilon = 0^+$ . Rewriting things now in the cosmological time t and setting  $\vec{x} = \vec{x}'$ , appropriate for a comoving detector, we have

$$y(\tau, \tau') = -4\left(\sinh\frac{H\Delta\tau}{2} - i\epsilon\right)^2 \tag{10}$$

Note that since we have set the comoving spatial separation to zero, the cosmological time  $\tau$  becomes the proper time along the detector's trajectory. We note that if more than two detectors are present, we cannot ignore the spatial coordinates from our calculations when two point function connecting these two points appear, due to their non-vanishing *mutual* spatial separation. Hence we will keep it below for our current purpose.

For a complex scalar field, the simplest field-detector coupling reads,

$$\mathcal{L}_{\text{int}} = -g(\tau)\mu(\tau)\phi^{\dagger}(x(\tau))\phi(x(\tau)) \tag{11}$$

Alike the fermions, e.g. [83], the quadratic coupling is necessary in order to make the interaction Hamiltonian hermitian. This means that the corresponding response function integrals will contain a product of two Wightman functions. Before moving forward, let us write the Wightman function of a conformally invariant complex scalar field. It can be obtained by setting m = 0 and  $\xi = 1/6$  in Eq. (9), and is given by

$$iG_C^+(x, x') = \frac{H^2}{4\pi^2} \left[ 4\sinh^2\left(\frac{H}{2}(\Delta\tau - i\epsilon)\right) + e^{H(\tau_1 + \tau_2)}r^2 \right]^{-1},$$
 (12)

where  $r = |\vec{x}_1 - \vec{x}_2|$  is the comoving separation. For a massless and minimally coupled scalar field, we have  $\nu = 3/2$  and hence Eq. (9) has no sensible limit. Thus the Wightman function in this case must be determined individually. For our present purpose, we will take the form derived in [57],

$$iG_{M}^{+}(x,x') = \frac{H^{2}}{16\pi^{2}} \left[ -\sinh^{2}\left(\frac{H}{2}(\Delta\tau - i\epsilon)\right) + e^{H(\tau_{1} + \tau_{2})}\left(\frac{Hr}{2}\right)^{2} \right]^{-1}$$

$$-\frac{H^{2}}{8\pi^{2}} \operatorname{Ei}\left[ -\frac{i\tilde{\epsilon}}{H}\left(-Hr + 2e^{-\frac{H(\tau_{1} + \tau_{2})}{2}}\sinh\left(\frac{H}{2}(\Delta\tau - i\epsilon)\right)\right) \right]$$

$$-\frac{H^{2}}{8\pi^{2}} \operatorname{Ei}\left[ -\frac{i\tilde{\epsilon}}{H}\left(Hr + 2e^{-\frac{H(\tau_{1} + \tau_{2})}{2}}\sinh\left(\frac{H}{2}(\Delta\tau - i\epsilon)\right)\right) \right] + \frac{H^{2}}{4\pi^{2}}$$

$$(13)$$

where Ei is the exponential integral function given by [84],

$$\operatorname{Ei}[z] = \int_{z}^{\infty} \frac{dt}{t} e^{-t} \tag{14}$$

In addition to the usual regulator  $\epsilon = 0^+$ , there is another positive infinitesimal parameter appearing above,  $\tilde{\epsilon} \ll H$ , in order to regularise the infrared divergences. Physically,  $\tilde{\epsilon}^{-1}$  represents the horizon scale at the onset of inflation. We refer our reader to [58] for detailed discussions.

# A. Complex scalar field coupled to two Unruh-DeWitt detectors

We now consider two Unruh-DeWitt detectors coupled to a complex scalar field. As of Eq. (3), the simplest interaction Hamiltonian reads for this composite system as

$$H_I = \sum_j g_j \mu_j(\tau_j) \phi^{\dagger}(x(\tau_j)) \phi(x(\tau_j))$$
(15)

where the index j runs for both the detectors, labeled as A and B. We explicitly expand the monopole moment of the detectors (introduced below Eq. (3)) in the Heisenberg picture as a function of the proper time as [85-87]

$$\mu_j(\tau_j) = |E_j\rangle\langle G_j|e^{i\omega_j\tau_j} + |G_j\rangle\langle E_j|e^{-i\omega_j\tau_j} \qquad \text{(no sum)}$$

G and E in the above expression stand respectively for the ground and excited levels of the detectors. For simplicity, we imagine both detectors to be identical so that  $\omega_j = \omega$  and  $g_j = g$ . We also assume that both the detectors and the scalar field are in their ground states initially, so that the initial state is given by

$$|\mathrm{in}\rangle = |0 \otimes G_A \otimes G_B\rangle$$
 (17)

Being a perfectly product state, it does not represent any entanglement initially. From now on, we shall suppress the tensor product symbol for the sake of notational brevity. The time evolution of this initial state in the interaction picture is given by

$$|\text{out}\rangle = U|\text{in}\rangle = Te^{-i\int d\tau_j H_I(t(\tau_j))}|0G_A G_B\rangle$$
 (18)

where T stands for time ordering. We make the perturbative expansion,  $U = I + U^{(1)} + U^{(2)} + \cdots$ , with

$$U^{(1)} = -i \int_{-\infty}^{\infty} d\tau_j \ H_I(t(\tau_j)) \tag{19}$$

$$U^{(2)} = -\int_{-\infty}^{\infty} d\tau_i \int_{-\infty}^{\tau} d\tau_j' H_I(t(\tau_i)) H_I(t'(\tau_j'))$$
 (20)

and so on. The density operator corresponding to the out state is given by

$$\rho = |\text{out}\rangle\langle\text{out}| = \rho^{(0)} + \rho^{(1)} + \rho^{(2)} + O(g^3)$$
(21)

where  $\rho^{(n)}$  is of the order of  $g^n$ . Also note that, since the initial state of the field is the vacuum, we have  $\rho^{(1)} = 0$  due to the vanishing one point function of the field. The two detectors interact with each other via the scalar field. The reduced density matrix of the two detectors is obtained by tracing out the field  $\phi$ 's degrees of freedom, resulting in the mixed density matrix

$$\rho_{AB} = \text{Tr}_{\phi} \rho = \begin{pmatrix} 1 - P_{AA} - P_{BB} & 0 & 0 & E^* \\ 0 & P_{AA} & P_{AB} & 0 \\ 0 & P_{AB} & P_{BB} & 0 \\ E & 0 & 0 & 0 \end{pmatrix}$$
 (22)

The basis of  $\rho_{AB}$  is  $|G_AG_B\rangle$ ,  $|G_AE_B\rangle$ ,  $|E_AG_B\rangle$  and  $|E_AE_B\rangle$ , and the matrix elements explicitly read,

$$P_{IJ} = g^2 \int d\tau_I \int d\tau_J' e^{-i\omega(\tau_I - \tau_J')} (iG^+(x_I, x_J'))^2 \qquad (I, J = A, B)$$
 (23)

$$E = -g^2 \int d\tau_A \int d\tau_B \ e^{i\omega(\tau_A + \tau_B)} (iG^+(x_A, x_B))^2$$
 (24)

where  $iG^+$  is the positive frequency Wightmann function.

Now we compute the negativity to quantify the entanglement between the two detectors represented by Eq. (22). The negativity of a bipartite state is defined as the absolute sum of the negative eigenvalues of  $\rho_{AB}^{T_A}$ , where  $\rho_{AB}^{T_A}$  is the partial transpose of  $\rho_{AB}$  with respect to the subspace of A, i.e.,  $(|i\rangle_A\langle n|\otimes |j\rangle_B\langle \ell|)^{T_A}:=|n\rangle_A\langle i|\otimes |j\rangle_B\langle \ell|$ . The partial transposed density matrix  $\rho_{AB}$  reads

$$(\rho_{AB})^{\mathrm{T}_{A}} = \begin{pmatrix} 1 - 2P & 0 & 0 & P_{AB} \\ 0 & P & E & 0 \\ 0 & E^{*} & P & 0 \\ P_{AB} & 0 & 0 & 0 \end{pmatrix}$$

$$(25)$$

where we have used  $P_{AA} = P_{BB} = P$ , owing to the identical nature of the detectors. The eigenvalues of Eq. (25) are given by

$$\lambda_{1} = \frac{1}{2} \left( 1 - 2P + \sqrt{(1 - 2P)^{2} + 4P^{2}} \right)$$

$$\lambda_{2} = \frac{1}{2} \left( 1 - 2P - \sqrt{(1 - 2P)^{2} + 4P^{2}} \right)$$

$$\lambda_{3} = P + |E| \qquad \lambda_{4} = P - |E|$$
(26)

Now we recall the fundamental result that a bipartite system which satisfies

$$|E| \ge P,\tag{27}$$

is entangled [6]. In this case, the negativity is defined as [88–90],

$$N = \max[0, |E| - P] \tag{28}$$

Therefore, for our present case we have

$$N = |E| - P \tag{29}$$

For initially separable detector states, a positive value of N following interaction with the scalar field suggests that the detectors become entangled finally. Negativity serves as a necessary and sufficient criterion for entanglement in two-qubit systems [6].

The transition integrals of Eq. (23), Eq. (24) are not convergent, owing to the integral over the variable  $\tau_+$ , Eq. (7). In order to regularise these integrals, one introduces a switching or window function, e.g. [57], and references therein. Such function effectively restricts the interaction time between the detectors. The most popular, which we will also be using, is the Gaussian window function,

$$g \to g(\tau) := ge^{-\tau^2/2\sigma^2} \tag{30}$$

in Eq. (23) and Eq. (24). This effective interaction profile ensures a smooth interaction transition. In de Sitter spacetime, two comoving detectors are causally disconnected if their comoving distance r satisfies

$$r > \frac{2\sinh H\sigma}{H},\tag{31}$$

This condition arises because the comoving causal length for each detector is given by

$$r_{\text{null}} = \int_{-\sigma}^{\sigma} \frac{d\tau}{a} = \frac{2\sinh H\sigma}{H}.$$
 (32)

Thus for two detectors initially in a separable state and satisfying the condition,

$$r > r_{\text{null}},$$
 (33)

the entanglement harvested can be attributed to the intrinsic entanglement of the scalar field, as local quantum measurements cannot generate entanglement between causally disconnected regions. Conversely, if  $r < r_{\text{null}}$ , the detectors are causally connected, allowing for direct causal interaction. In this case, attributing the observed entanglement as solely arising from the non-local correlations

of the scalar field becomes less straightforward due to the possibility of the local interactions.

As we have stated above, if we do not use a switching function, the interaction persists indefinitely, leading to divergences in the transition probability due to the infinite integration over time. This also results in the appearance of the logarithmic secular growth for a massless minimally coupled scalar field, e.g. [81, 91] and references therein. To address these divergences and extract physically meaningful quantities, one alternative approach would be to compute transition probabilities per unit proper time. This is done by redefining the temporal variables as of Eq. (7) and then normalising the transition integrals by dividing it by  $\lim_{\tau_+ \to \infty} \tau_+$ . This prescription ensures a well-defined transition rate, preventing unphysical divergences. However while it does so, it is not difficult to verify that the absence of a switching function still leads to ill-defined energy eigenstates and density matrix elements. Therefore, introducing a switching function seems to be essential to overcome these effects and ensure well defined transition rates and density matrix eigenvalues. Nevertheless, a plausible critique to the introduction of such function still will be, in a cosmological scenario, turning on or off the interaction can never be in our hand. In fact it might be possible that the interaction remains omnipresent, as is always the case in a non-equilibrium scenario.

With these, are now ready to go into the computation of entanglement generation due to field-detectors couplings.

### III. COMPUTATION OF THE TRANSITION INTEGRALS AND THE NEGATIVITY

# A. A complex conformal scalar field

Let us begin with a conformally invariant complex scalar field in the conformal vacuum, coupled to two Unruh-DeWitt detectors. Substituting Eq. (12), Eq. (30) into Eq. (23) and Eq. (24), we have the following transition integrals

$$P_{IJ} = g^2 \int d\tau_I d\tau_J' \ e^{-(\tau_I^2 + {\tau'}_J^2)/2\sigma^2} e^{-i\omega(\tau_I - {\tau'}_J)} (iG_C^+(x_I, x_J'))^2 \qquad (I, J = A, B)$$

$$E = -g^2 \int d\tau_A d\tau_B' \ e^{-(\tau_A^2 + {\tau'}_B^2)/2\sigma^2} e^{-i\omega(\tau_A + {\tau'}_B)} (iG_C^+(x_A, x_B'))^2, \qquad (34)$$

By substituting these expressions into Eq. (29), we can determine the negativity for the two identical detectors. In order to compute the negativity, it is necessary to evaluate  $P_{IJ}$  for I = J (i.e. the same detector), where the spatial separation is set to zero r = 0. We have for identical detectors

$$P_{AA} = P_{BB} = P(r = 0) = \frac{g^2 H^4}{256\pi^4} \int d\tau \int d\tau' \frac{e^{-\frac{\tau^2 + \tau'^2}{2\sigma^2}} e^{-i\omega(\tau - \tau')}}{\left[\sinh\left(H\left(\frac{\tau - \tau'}{2} - i\epsilon\right)\right)\right]^4}$$
(35)

On rewriting this integral in terms of temporal variables defined in Eq. (7), we have

$$P = \frac{H^4 g^2}{256\pi^2} \int_{-\infty}^{\infty} d\tau_+ \ e^{-\tau_+^2/\sigma^2} \int_{-\infty}^{\infty} d(\Delta \tau) \frac{e^{-\Delta \tau^2/\sigma^2} e^{-2i\omega \Delta \tau}}{\left[\sinh(H(\Delta \tau - i\epsilon))\right]^4},$$
 (36)

which, after rescaling the temporal variables, and defining  $H\sigma = h$ , is rewritten as

$$P = \frac{H^2 g^2 h^2}{256\pi^4} \int_{-\infty}^{\infty} dx \ e^{-x^2} \int_{-\infty}^{\infty} dy \frac{e^{-y^2 - 2i\omega\sigma y}}{\left[\sinh(h(y - i\epsilon))\right]^4} = \frac{H^2 g^2 h^2}{256\pi^{7/2}} \int_{-\infty}^{\infty} dy \frac{e^{-y^2 - 2i\omega\sigma y}}{\left[\sinh(h(y - i\epsilon))\right]^4}$$
(37)

Likewise, the second of Eq. (34) gives,

$$E = -\frac{H^2 g^2 h^2}{128\pi^4} \int_{-\infty}^{\infty} dx \ e^{-x^2 + 2i\omega\sigma x} \int_{-\infty}^{\infty} dy \frac{e^{-y^2}}{\left[\sinh^2(h(y - i\epsilon)) - e^{2hx}(Hr/2)^2\right]^2}$$
(38)

We could not evaluate Eq. (37) and Eq. (38) in closed forms and have found them numerically. However, before we do that, we need to cast them into a more tractable form, as described in Appendix A. The reformulated integrals are respectively given by

$$P = \frac{H^2 g^2 h^2 e^{-\omega^2 \sigma^2}}{96\pi^3} \int_0^\infty dk \ e^{-k^2} k^3 \frac{\cosh\frac{k\pi}{h} (1 - \frac{2h\omega\sigma}{\pi})}{\sinh\frac{k\pi}{h}}$$
(39)

$$E = -\frac{H^2 g^2}{64\pi^{3/2}} \int_{-\infty}^{\infty} dx \ e^{-x^2 + 2i\omega\sigma x} \int_{-\infty}^{\infty} dk \ e^{-k^2} \frac{\sin\left(\frac{2k\ln b}{h}\right) \cosh\frac{2\pi k}{h}}{a\left(1 + a^2h^2\right)\left(1 - e^{\frac{2\pi k}{h}}\right)} \left(\frac{h}{\ln b} + 2ik\right)$$
(40)

where we have abbreviated,  $a = e^{hx}r/2\sigma$  and  $b = ah + \sqrt{a^2h^2 + 1}$ . Following [57], we next assume the following parameter ranges for asymptotic numerical analysis:

$$\omega \sigma \gg 1, \ \frac{\pi}{h} \gg 1, \ \text{and} \ \frac{r}{2\sigma} \gg 1$$
 (41)

The first simply states that the characteristic time scale associated with the detectors are much small compared to their interaction time. Since  $h = H\sigma$ , the second condition implies that the interaction time scale is much small compared to that of the inflation. The third is an outcome of the fact that  $h \ll 1$ , and it indicates that the two detectors are causally disconnected. For a detailed calculation of the asymptotic analysis, we refer the reader to Appendix B.

After evaluating Eq. (39) and Eq. (40) numerically, we have computed the entanglement negativity using Eq. (29). Fig. 1 shows the behaviour of the same, with respect to the dimensionless parameters  $r/2\sigma$  (detectors' separation) and  $\omega\sigma$  (energy gap), for various values of the coupling strength g and interaction duration  $h = H\sigma$ . As can be seen, the negativity can be nonzero even for super-horizon separations ( $r/2\sigma > 1$ ), revealing persistent non-local correlations in the conformal vacuum. Increasing h suppresses entanglement due to accumulated local noise, while stronger coupling g enhances the entanglement harvesting. A notable feature is the non-monotonic dependence

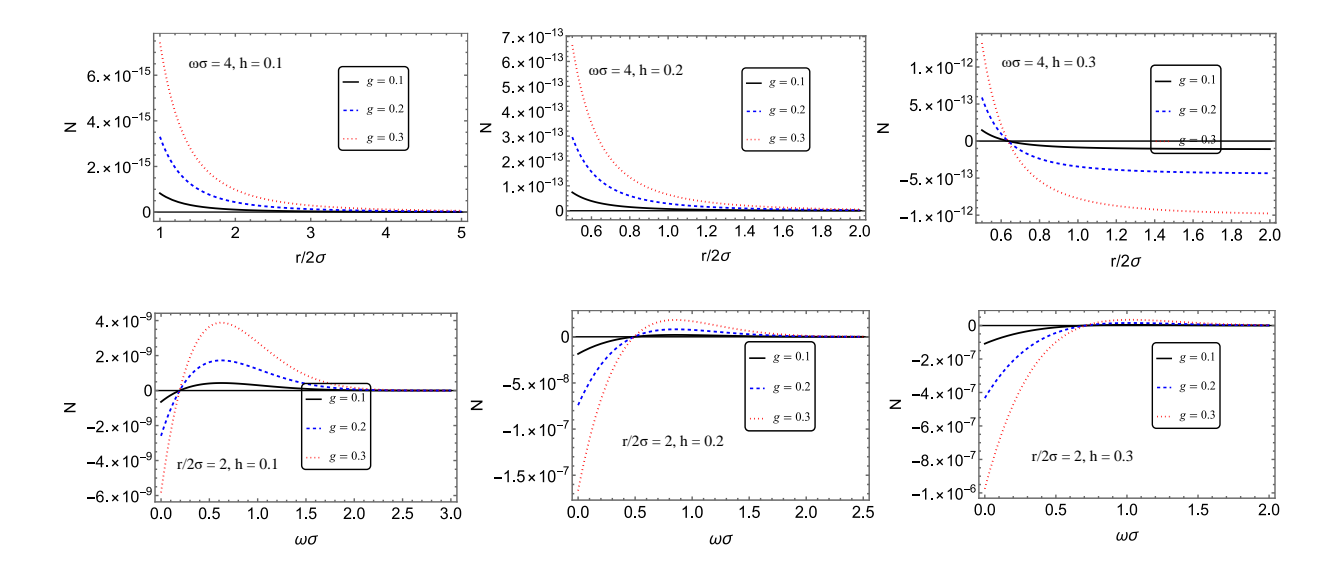


FIG. 1. Negativity between two Unruh-DeWitt detectors coupled to a conformally invariant, massless complex scalar field as a function of the dimensionless parameters  $r/2\sigma$  and  $\omega\sigma$ , for various values of coupling g and interaction duration  $h = H\sigma$ . Note that a negative N implies that the physical negativity is zero, and hence no entanglement between the detectors.

on  $\omega\sigma$ : negativity initially increases due to better spectral overlap with field modes, but eventually decreases as high-frequency modes contribute weakly to long-range correlations due to their shorter wavelengths. This behaviour parallels the threshold phenomenon discussed in [92], where entanglement between spatially separated regions vanishes beyond a critical scale, emphasising the spectral and spatial limitations in accessing vacuum entanglement.

# B. The massless minimally coupled scalar field

Let us now come to the case of a massless, minimal scalar field, for which the Wightman function is given by Eq. (13). Substituting Eq. (13) into Eq. (23) and Eq. (24), we may compute  $P_{IJ}$  and E, similar to the earlier case of the conformal scalar. Let us first evaluate  $P_{IJ}$  for I = J, where the spatial separation between the detectors is zero, i.e., r = 0, for which Eq. (13) becomes

$$iG_M^+(x,x') = \frac{H^2}{16\pi^2} \left[-\sinh^2 H(y-i\epsilon)\right]^{-1} - \frac{H^2}{4\pi^2} \operatorname{Ei}\left[-\frac{2i\tilde{\epsilon}}{H}e^{-H\tau_+}\sinh\left(H(y-i\epsilon)\right)\right] + \frac{H^2}{4\pi^2}$$
(42)

We have

$$P = \frac{H^2 g^2 h^2}{16\pi^4} \int_{-\infty}^{\infty} dx \ e^{-x^2} \int_{-\infty}^{\infty} dy \ e^{-y^2 - 2i\omega\sigma y} \left[ \frac{1}{4\sinh^2(h(y - i\epsilon))} + \text{Ei} \left[ -\frac{2i\tilde{\epsilon}}{H} e^{-hx} \sinh(h(y - i\epsilon)) \right] - 1 \right]^2$$
(43)

Upon expanding the square bracket and simplifying a bit, we have (see Appendix B for detail)

$$P = \frac{H^{2}g^{2}h^{2}}{8\pi^{3}} \int_{0}^{\infty} dk \ e^{-k^{2}}k \frac{\cosh\frac{k\pi}{h}(1 - 2h\omega\sigma/\pi)}{\sinh\frac{k\pi}{h}} + \frac{H^{2}g^{2}h^{2}}{16\pi^{3}}e^{-\omega^{2}\sigma^{2}} + \frac{H^{2}g^{2}h^{2}e^{-\omega^{2}\sigma^{2}}}{96\pi^{3}} \int_{0}^{\infty} dk \ e^{-k^{2}}k^{3}\frac{\cosh\frac{k\pi}{h}(1 - 2h\omega\sigma/\pi)}{\sinh\frac{k\pi}{h}} + \frac{g^{2}H^{2}h^{2}e^{-\omega^{2}\sigma^{2}}}{16\pi^{3}} \left[ \left( \gamma + \ln\frac{2\tilde{\epsilon}}{H} + \ln\left(h(\omega + \epsilon)\right) + \frac{h^{2}}{2} \right)^{2} + \frac{h^{2}}{2} \right] + \frac{g^{2}H^{2}h^{2}e^{-\omega^{2}\sigma^{2}}}{16\pi^{3}} \left( \gamma + \ln\frac{2\tilde{\epsilon}}{H} + \ln\left(h(\omega + \epsilon)\right) + \frac{h^{2}}{2} \right) + \frac{g^{2}H^{2}e^{-\omega^{2}\sigma^{2}}}{64\pi^{3}\Omega^{2}} \left( \gamma + \ln\frac{2\tilde{\epsilon}}{H} + \ln\left(h(\omega + \epsilon)\right) \right)$$

$$(44)$$

Likewise, we find matrix element E using Eq. (24) and Eq. (13) as

$$E = -g^{2} \int_{-\infty}^{\infty} dx \ e^{-x^{2}+2i\omega\sigma x} \int_{-\infty}^{\infty} dy \ e^{-y^{2}} \left[ \frac{h^{2}}{16\pi^{2}(-\sinh^{2}(h(y-i\epsilon)) + e^{2hx}(hr/2\sigma)^{2})} + \frac{h^{2}}{4\pi^{2}} \right]$$

$$- \frac{h^{2}}{8\pi^{2}} \text{Ei} \left[ -\frac{i\tilde{\epsilon}}{H} \left( -Hr + 2e^{-hx}\sinh(h(y-i\epsilon)) \right) \right] - \frac{h^{2}}{8\pi^{2}} \text{Ei} \left[ -\frac{i\tilde{\epsilon}}{H} \left( Hr + 2e^{-hx}\sinh(h(y-i\epsilon)) \right) \right] \right]^{2}$$

$$= -\frac{H^{4}g^{2}h^{2}}{16\pi^{4}} \int_{-\infty}^{\infty} dx \ e^{-x^{2}+2i\omega\sigma x} \int_{-\infty}^{\infty} dy \ e^{-y^{2}} \left[ \frac{1}{4(-\sinh^{2}(h(y-i\epsilon)) + e^{2hx}(\frac{hr}{2\sigma})^{2})} + 1 \right]$$

$$- \frac{1}{2} \text{Ei} \left[ -\frac{i\tilde{\epsilon}}{H} \left( -Hr + 2e^{-hx}\sinh(h(y-i\epsilon)) \right) \right] - \frac{1}{2} \text{Ei} \left[ -\frac{i\tilde{\epsilon}}{H} \left( Hr + 2e^{-hx}\sinh(h(y-i\epsilon)) \right) \right]^{2},$$

$$(45)$$

which after simplifying a bit, reads (see Appendix B for details)

$$E = -\frac{g^2 H^2 h^2 e^{-\omega^2 \sigma^2}}{16\pi^{7/2}} \int_{-\infty}^{\infty} dy \ e^{-y^2} \left[ \frac{1}{4 \left( h^2 (y - i\epsilon)^2 + e^{i2h\omega\sigma} (hr/2\sigma)^2 \right)} + 1 + \gamma + \frac{1}{2} \left( \ln \left[ \frac{i\tilde{\epsilon}}{H} (-Hr + 2e^{-ih\omega\sigma} h(y - i\epsilon)) \right] + \ln \left[ \frac{i\tilde{\epsilon}}{H} (Hr + 2e^{-ih\omega\sigma} h(y - i\epsilon)) \right] \right) \right]$$

$$(46)$$

We could not simplify Eq. (44) and Eq. (46) any further analytically. Plugging these expressions next into Eq. (29), we have numerically computed the entanglement negativity as earlier and have investigated its variation in Fig. 2, keeping the infrared regulator fixed at  $\tilde{\epsilon}/H = e^{-20}$ , following [57]. Just like the previous case of the conformal scalar, we note that the negativity remains nonzero

even when the detectors are separated beyond their causal horizon  $(r/2\sigma > 1)$ , demonstrating the presence of long-range correlations in the minimally coupled vacuum. The negativity decreases with increasing interaction duration  $(h = H\sigma)$  and detector energy gap  $(\omega\sigma)$ . Thus, as earlier, we see that longer interactions suppress entanglement due to local noise, while larger energy gaps reduce the detectors' sensitivity to low-frequency (and hence long wavelength) modes that mediate entanglement. We also note qualitative and quantitative differences in Fig. 2 from the conformally coupled scalar case shown in Fig. 1. In particular, for the minimally coupled scalar field, while the harvested entanglement may decay more rapidly with increasing separation in some regimes, the negativity remains strictly positive throughout the parameter space examined and, in fact, can surpass that of the conformal case at larger separations and longer interaction durations (compare the second row of Fig. 1 and Fig. 2). This highlights the enhanced robustness of entanglement harvesting in the minimal case, likely due to the infrared amplification of long-range correlations characteristic of the minimally coupled field.

An important distinction emerges when comparing our results for the minimally coupled complex scalar with previous studies involving real scalars and linear couplings. Notably, [57] demonstrated that for a real scalar field in de Sitter spacetime, entanglement becomes undetectable once the detector separation exceeds the Hubble horizon (i.e.,  $r/2\sigma \gtrsim 1$ ), consistent with the onset of classical behaviour. In contrast, our analysis shows that for a complex scalar field with Hermitian quadratic coupling  $(\phi^{\dagger}\phi)$ , the negativity remains nonzero even in the infrared regime  $(\omega\sigma \ll 1)$ , and persists across super-horizon separations  $(r/2\sigma \gtrsim 1)$ . This robustness arises from both the infrared enhancement characteristic of the minimally coupled field and the amplification of non-local correlations induced by the nonlinear interaction. These results suggest that entanglement harvesting is more resilient in scenarios involving complex fields and nonlinear couplings, underscoring the sensitivity of observable quantum correlations to the nature of the field and its interaction with detectors.

## IV. CONCLUSION

In this work, we analysed entanglement harvesting by two identical, comoving Unruh-DeWitt detectors in de Sitter spacetime, interacting with each other via either a conformally invariant or a minimally coupled massless complex scalar field. We computed the negativity as a measure of entanglement and studied its dependence on detector separation, energy gap, and interaction duration.

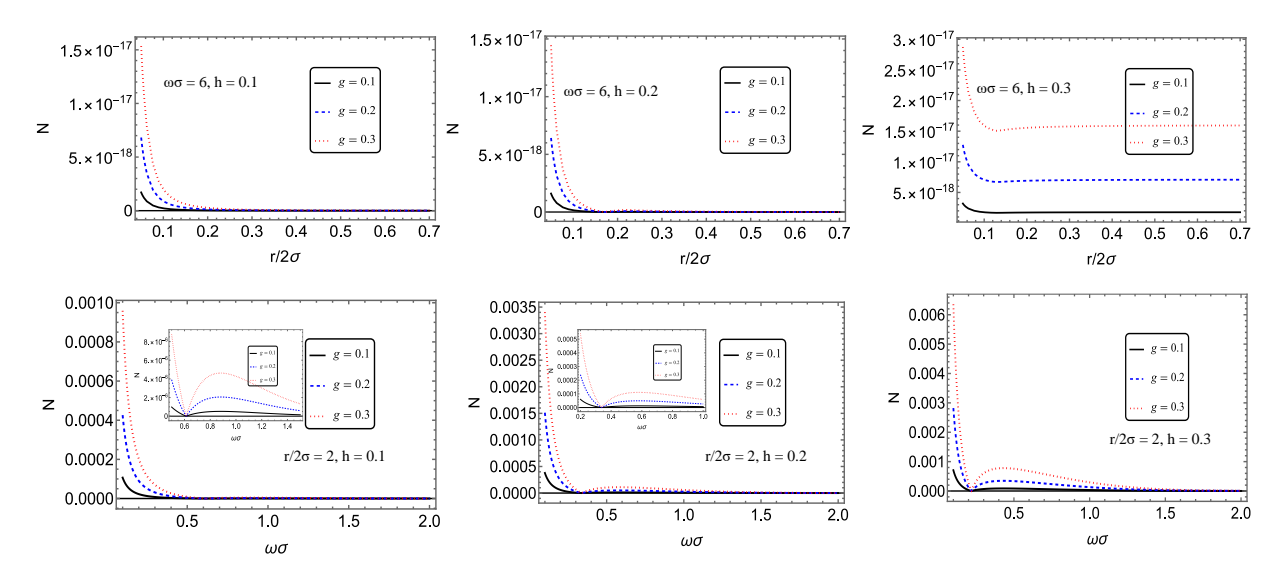


FIG. 2. Negativity between two Unruh-DeWitt detectors coupled to a massless minimally coupled complex scalar field as a function of the dimensionless parameters  $r/2\sigma$  and  $\omega\sigma$ , for different values of the coupling g and interaction duration  $h = H\sigma$ , while keeping the infrared regulator fixed at  $\tilde{\epsilon}/H = e^{-20}$ .

Our results show that for the conformally coupled scalar field, entanglement can be harvested even at super-horizon separations, highlighting the persistence of non-local correlations in the de Sitter vacuum. However, the degree of entanglement is sensitive to both the energy gap and the interaction duration. In contrast, the massless minimally coupled complex scalar field exhibits a qualitatively different behaviour: the negativity remains strictly positive throughout the parameter space considered, including at super-horizon separations. This indicates that some entanglement is always harvested, although its magnitude also decreases with increasing energy gap and interaction time. Notably, at larger separations and longer interaction durations, the harvested entanglement can surpass that of the conformal case. This enhancement can be attributed to the infrared amplification of long-wavelength field correlations in the minimally coupled field. Importantly, in both cases, the entanglement decays smoothly with increasing separation or energy gap, without exhibiting a sharp cutoff at the horizon scale—unlike the abrupt suppression observed in earlier studies involving real scalar fields with linear coupling (cf. discussion towards the end of the preceding section).

These findings underline that entanglement harvesting is shaped not only by causal structure, but also by the quantum nature of the field and the choice of coupling. They also suggest that features such as the persistence or suppression of negativity carry imprints of the underlying field theory, offering a window into the entanglement structure of quantum fields in curved spacetime.

Future investigations could extend this analysis to other types of fields and couplings, explore non-inertial detector trajectories, or consider decoherence effects. In particular, studying the decoherence dynamics between detectors—whether initially entangled or unentangled—may provide further insight into the transition from quantum to classical behaviour in cosmological environments. Extensions incorporating critical slowing down [93, 94] in multi-detector settings also present compelling directions for future research.

### Appendix A: A brief sketch of the computation of Eq. (39) and Eq. (40)

Following [57], we wish to sketch below some detail for the simplification of Eq. (37) and Eq. (38), leading to Eq. (39), Eq. (40). For example, using

$$e^{-y^2} = \frac{1}{\sqrt{\pi}} \int_{-\infty}^{\infty} dk \ e^{-k^2 + 2iky}$$
 (A1)

in Eq. (37), we obtain

$$P = \frac{H^2 g^2 h^2}{256\pi^4} \int_{-\infty}^{\infty} dk \ e^{-(k+\omega\sigma)^2} \int_{-\infty}^{\infty} dy \frac{e^{2iky}}{\left[\sinh\left(h(y-i\epsilon)\right)\right]^4}$$

$$= \frac{H^2 g^2 h^2}{256\pi^4} \int_{-\infty}^{\infty} dk \ e^{-(k+\omega\sigma)^2} \int_{-\infty}^{\infty} dy \sum_{n=-\infty}^{\infty} \frac{e^{2iky}}{\left(y-i\epsilon - \frac{i\pi n}{h}\right)^4}$$
(A2)

it has  $4^{th}$  order poles 4 at  $(i\pi n/h + i\epsilon)$ . Let us consider the integral

$$A_1(k) = \int_{-\infty}^{\infty} dy \sum_{n = -\infty}^{\infty} \frac{e^{2iky}}{(y - i\epsilon - \frac{i\pi n}{h})^4}$$
(A3)

This integral can be solved by choosing the contour Fig. 3. The residue at  $i\epsilon + i\pi n$  is

$$\frac{1}{3!} \lim_{\epsilon \to 0} \left( \lim_{y \to \frac{i\pi n}{h} + i\epsilon} \frac{d^3}{dy^3} (e^{2iky}) \right) = -\frac{8i}{6} e^{-\frac{2k\pi n}{h}} k^3 \tag{A4}$$

On substituting Eq. (A4) in Eq. (A3), we obtain

$$A_1(k) = \frac{8\pi k^3}{3(1 - e^{-2\pi k/h})} \tag{A5}$$

Finally, on substituting Eq. (A5) into Eq. (A2), we get

$$P = \frac{H^2 g^2 h^2}{96\pi^3} \int_{-\infty}^{\infty} dk \ k^3 \frac{e^{-(k+\omega\sigma)^2}}{1 - e^{-\frac{2\pi k}{h}}} = \frac{H^2 g^2 h^2 e^{-\omega^2 \sigma^2}}{96\pi^3} \int_0^{\infty} dk \ e^{-k^2} k^3 \frac{\cosh\left(\frac{k\pi}{h}(1 - \frac{2h\omega\sigma}{\pi})\right)}{\sinh\frac{k\pi}{h}}$$
(A6)

Next, in order to compute E, we substitute Eq. (A1) into Eq. (38) to obtain

$$E = -\frac{H^2 g^2 h^2}{256\pi^{5/2}} \int_{-\infty}^{\infty} dx e^{-x^2 + 2i\omega\sigma x} \int_{-\infty}^{\infty} dk \ e^{-k^2} \int_{-\infty}^{\infty} dy \frac{e^{2iky}}{[-\sinh^2\left(h(y-i\epsilon)\right) + e^{2hx}(hr/2\sigma)^2]^2}$$

$$= -\frac{H^2 g^2}{128\pi^{5/2}} \int_{-\infty}^{\infty} dx \ e^{-x^2 + 2i\omega\sigma x} \int_{-\infty}^{\infty} dk \ e^{-k^2} \int_{0}^{\infty} dy \frac{e^{2iky}}{\left[\frac{\sinh^2\left(h(y-i\epsilon)\right)}{h^2} - e^{2hx}(r/2\sigma)^2\right]^2}$$
(A7)

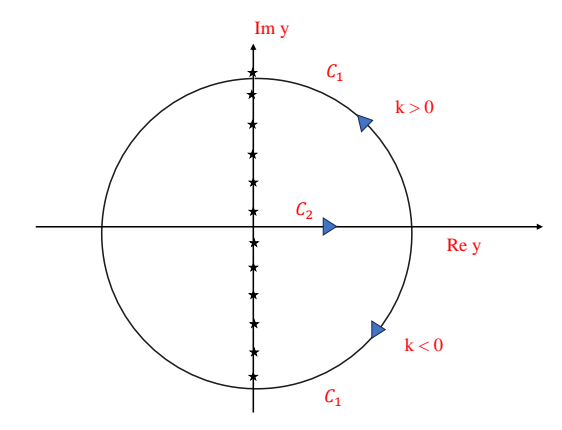


FIG. 3. The integration contour for  $A_1(k)$ , Eq. (A3). The radius of the contour  $C_1$  is taken to be infinite.

Let us now evaluate

$$A_2(k) = \int_0^\infty dy \frac{e^{2iky}}{\left\lceil \frac{\sinh^2\left(h(y-i\epsilon)\right)}{h^2} - e^{2hx}(r/2\sigma)^2 \right\rceil^2}$$
(A8)

Defining  $a = e^{hx}r/2\sigma$ , we rewrite the above equation as

$$A_2(k) = \frac{1}{2a} \int_0^\infty dy \ e^{2iky} \left( \frac{1}{\frac{\sinh(h(y-i\epsilon))}{h} - a} - \frac{1}{\frac{\sinh(h(y-i\epsilon))}{h} + a} \right)^2$$
 (A9)

The above integral can be rewritten as

$$A_2(k) = \frac{1}{2a(ah + \frac{1}{b})^2} \int_0^\infty dy \ e^{2iky} \sum_{n = -\infty}^\infty \left[ \frac{1}{(y - y_1)^2} + \frac{1}{(y - y_2)^2} - \frac{2}{(y - y_1)(y - y_2)} \right]$$
(A10)

where

$$y_1 = \left(i\epsilon + \frac{\ln b}{h} + \frac{in\pi}{h}\right), \ y_2 = \left(i\epsilon - \frac{\ln b}{h} + \frac{in\pi}{h}\right), \ b = ah + \sqrt{a^2h^2 + 1}. \tag{A11}$$

Putting everything together, and choosing the contour depicted in Fig. 4, we obtain after a little algebra

$$A_2(k) = \frac{2\pi \sin\left(\frac{2k \ln b}{h}\right) \cosh\frac{2\pi k}{h}}{a(1+a^2h^2)(1-e^{\frac{2\pi k}{h}})} \left(\frac{h}{\ln b} + 2ik\right)$$
(A12)

Finally, upon substituting Eq. (A12) into Eq. (A7), we have

$$E = -\frac{H^2 g^2}{64\pi^{3/2}} \int_{-\infty}^{\infty} dx \ e^{-x^2 + 2i\omega\sigma x} \int_{-\infty}^{\infty} dk \ e^{-k^2} \frac{\sin\left(\frac{2k\ln b}{h}\right) \cosh\frac{2\pi k}{h}}{a(1+a^2h^2)\left(1 - e^{\frac{2\pi k}{h}}\right)} \left(\frac{h}{\ln b} + 2ik\right)$$
(A13)

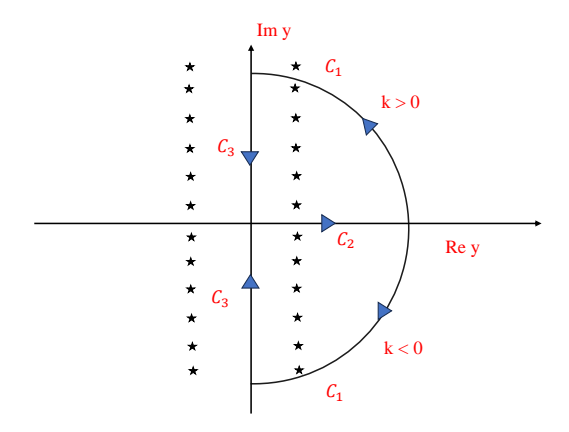


FIG. 4. The integration contour for  $A_2(k)$ , Eq. (A10). The radius of the contour  $C_1$  is taken to be infinite.

## Appendix B: Asymptotic analysis of integrals Eq. (37), Eq. (38), Eq. (44) and Eq. (45)

We introduce the following change of variables:

$$\omega \sigma \equiv \Omega, \quad \frac{h}{\pi} \equiv \tilde{h} \quad \text{and} \quad \frac{r}{2\sigma} \equiv \tilde{r}$$
 (B1)

First, let us rewrite Eq. (37) and Eq. (38) respectively as,

$$P = \frac{H^2 g^2 \tilde{h}^2 e^{-\Omega^2}}{96\pi} \int_0^\infty dk \ e^{-k^2} k^3 \frac{\cosh\frac{k(1-2\tilde{h}\Omega)}{\tilde{h}}}{\sinh\frac{k}{\tilde{L}}},\tag{B2}$$

and,

$$E = -\frac{H^2 g^2}{64\pi^{3/2}} \int_{-\infty}^{\infty} dx \ e^{-x^2 + 2i\Omega x} \int_{-\infty}^{\infty} dk \ e^{-k^2} \frac{\sin\left(\frac{2k}{\pi \tilde{h}} \ln b\right) \cosh\frac{2k}{\tilde{h}}}{a(1 + a^2 \tilde{h}^2 \pi^2)(1 - e^{\frac{2k}{\tilde{h}}})} \left(\frac{\tilde{h}\pi}{\ln b} + 2ik\right), \tag{B3}$$

where a and b are defined as

$$a = e^{\tilde{h}\pi x}\tilde{r}$$
 and  $b = a\pi\tilde{h} + \sqrt{a^2\tilde{h}^2\pi^2 + 1}$  (B4)

We evaluated the integral in Eq. (B2) numerically. Next, following [57], we proceed to evaluate Eq. (B3) by first rewriting the approximations in Eq. (41) in terms of the new variables introduced in Eq. (B1):

$$\Omega \gg 1, \qquad \frac{1}{\tilde{h}} \gg 1 \text{ (or } \tilde{h} \ll 1) \qquad \text{and} \qquad \tilde{r} \gg 1$$
 (B5)

Using these approximations, we evaluate the integral in equation Eq. (B3) via the saddle point method. Consider the integral

$$I = \int_{-\infty}^{\infty} dx \, e^{-x^2 + 2i\Omega x} F(x), \quad \text{with} \quad \Omega \gg 1,$$
 (B6)

The maximum of the phase of the exponential,  $-x^2 + 2i\Omega x$  is located at  $x = i\Omega$ , i.e. on the imaginary axis. Expanding the phase around this maximum, we have

$$I \approx e^{-\Omega^2} F(i\Omega) \int_{-\infty}^{\infty} dx \, e^{-(x-i\Omega)^2} = \sqrt{\pi} \, e^{-\Omega^2} F(i\Omega). \tag{B7}$$

We now rewrite Eq. (B3) as

$$E = -\frac{H^2 g^2 e^{-\Omega^2}}{64\pi} \int_{-\infty}^{\infty} dk \, \frac{e^{-k^2} \sin\left(\frac{2k}{\pi\tilde{h}} \ln b(i\Omega)\right) \cosh\frac{2k}{\tilde{h}}}{a(i\Omega) \left(1 + \pi^2 \tilde{h}^2 \ln a(i\Omega)\right) \left(1 - e^{2k/\tilde{h}}\right)} \left(\frac{\pi\tilde{h}}{\ln b(i\Omega)} + 2ik\right), \tag{B8}$$

where  $a(i\Omega)$  and  $b(i\Omega)$  denote the values of the functions a and b evaluated at the saddle point  $x = i\Omega$ . We further rewrite Eq. (B8) as

$$E = -\frac{H^2 g^2}{64\pi} e^{-\Omega^2} \int_{-\infty}^{\infty} dk \frac{e^{-k^2 \sin\left(\frac{2k}{\pi\tilde{h}}\log\left(e^{i\tilde{h}\pi\Omega}\tilde{r}\tilde{h} + \sqrt{1 + (e^{i\tilde{h}\pi\Omega}\tilde{r})^2\pi^2}\right)\right) \cosh\frac{2k}{\tilde{h}}}}{e^{i\tilde{h}\pi\Omega}\tilde{r}\left(1 + (e^{i\tilde{h}\pi\Omega}\tilde{r})^2\pi^2\right)\left(1 - e^{2k/\tilde{h}}\right)}$$
(B9)

We integrate the above equation using the contour shown in Fig. 5. The integral is evaluated by summing the residues at the poles  $k_n = i\pi n\tilde{h}$  for n < 0, which arise from the zeros of the denominator  $1 - e^{2k/\tilde{h}} = 0$ . The residue at each pole simplifies to

$$\operatorname{Res}_{k=k_n} f(k) \approx \frac{i\tilde{h}}{2} \frac{\sinh\left(2n\log\left(e^{i\tilde{h}\pi\Omega}\tilde{r}\tilde{h} + \sqrt{1 + (e^{i\tilde{h}\pi\Omega}\tilde{r})^2\pi^2}\right)\right)}{e^{i\tilde{h}\pi\Omega}\tilde{r}\left(1 + (e^{i\tilde{h}\pi\Omega}\tilde{r})^2\pi^2\right)}$$
(B10)

This yields

$$E \approx -\frac{H^2 g^2 \tilde{h}}{128} e^{-\Omega^2} \frac{\coth\left(\log\left(e^{i\tilde{h}\pi\Omega} \tilde{r}\tilde{h} + \sqrt{1 + (e^{i\tilde{h}\pi\Omega} \tilde{r})^2 \pi^2}\right)\right)}{e^{i\tilde{h}\pi\Omega} \tilde{r}\left(1 + (e^{i\tilde{h}\pi\Omega} \tilde{r})^2 \pi^2\right)}$$
(B11)

Furthermore, we numerically computed the value of Eq. (B11) and the integral in Eq. (B2), and subsequently obtained the negativity for the conformal scalar field using Eq. (29). See main text for the same.

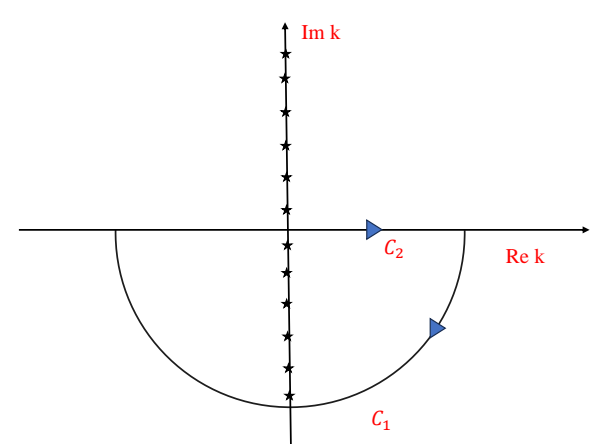


FIG. 5. The integration contour for Eq. (B9).

We next proceed to analyse the integrals Eq. (44) and Eq. (45) using the approximation specified in Eq. (41) (Eq. (B1)). We begin with Eq. (44), which can be expanded as

$$P = \frac{g^{2}H^{2}h^{2}}{256\pi^{4}} \int_{-\infty}^{\infty} dx \ e^{-x^{2}} \int_{-\infty}^{\infty} dy \frac{e^{-y^{2}-2i\omega\sigma y}}{\left[\sinh(h(y-i\epsilon))\right]^{4}}$$

$$+ \frac{g^{2}H^{2}h^{2}}{16\pi^{4}} \int_{-\infty}^{\infty} dx \ e^{-x^{2}} \int_{-\infty}^{\infty} dy \ e^{-y^{2}-2i\omega\sigma y} - \frac{g^{2}H^{2}h^{2}}{64\pi^{4}} \int_{-\infty}^{\infty} dx \ e^{-x^{2}} \int_{-\infty}^{\infty} dy \frac{e^{-y^{2}-2i\omega\sigma y}}{\sinh(h(y-i\epsilon))}$$

$$+ \frac{g^{2}H^{2}h^{2}}{16\pi^{4}} \int_{-\infty}^{\infty} dx \ \int_{-\infty}^{\infty} dy \ e^{-x^{2}-y^{2}-2i\omega\sigma y} \left[ \text{Ei} \left( -\frac{2i\tilde{\epsilon}}{H} e^{-hx} \sinh(h(y-i\epsilon)) \right) \right]^{2}$$

$$- \frac{g^{2}H^{2}h^{2}}{16\pi^{4}} \int_{-\infty}^{\infty} dx \ \int_{-\infty}^{\infty} dy \ e^{-x^{2}-y^{2}-2i\omega\sigma y} \text{Ei} \left( -\frac{2i\tilde{\epsilon}}{H} e^{-hx} \sinh(h(y-i\epsilon)) \right)$$

$$+ \frac{g^{2}H^{2}h^{2}}{64\pi^{4}} \int_{-\infty}^{\infty} dx \ \int_{-\infty}^{\infty} dy \ e^{-x^{2}-y^{2}-2i\omega\sigma y} \frac{\text{Ei} \left( -\frac{2i\tilde{\epsilon}}{H} e^{-hx} \sinh(h(y-i\epsilon)) \right)}{\left[ \sinh(h(y-i\epsilon)) \right]^{2}}$$

$$(B12)$$

We solve the above expression term by term. The first term in Eq. (B12) is identical to Eq. (37), which has been solved earlier and is given by Eq. (A6). The second term can be evaluated using Gaussian integral,

$$\frac{g^2 H^2 h^2}{16\pi^4} \int_{-\infty}^{\infty} dx \, e^{-x^2} \int_{-\infty}^{\infty} dy \, e^{-y^2 - 2i\omega\sigma y} = \frac{g^2 H^2 h^2}{16\pi^3} e^{-\omega^2 \sigma^2}$$
 (B13)

The third term can be evaluated in a manner similar to Eq. (37), as shown in Appendix A. We obtain

$$-\frac{g^2 H^2 h^2}{64\pi^4} \int_{-\infty}^{\infty} dx \, e^{-x^2} \int_{-\infty}^{\infty} dy \, \frac{e^{-y^2 - 2i\omega\sigma y}}{\sinh(h(y - i\epsilon))} = \frac{g^2 H^2}{8\pi^3} \int_{0}^{\infty} dk \, e^{-k^2} k \, \frac{\cosh\left(\frac{\pi k}{h}\left(1 - \frac{2h\omega\sigma}{\pi}\right)\right)}{\sinh\frac{\pi k}{h}}$$
(B14)

Furthermore, to solve the remaining terms, we use the following approximation for the exponential integral function [84]:

$$\operatorname{Ei}[-z] \approx -\gamma - \ln z, \quad \text{for } z \ll 1,$$
 (B15)

Using the approximation Eq. (B15) along with the saddle-point method discussed earlier in this Appendix to evaluate the integral I, Eq. (B7), we can compute the remaining terms, which are given by

$$\frac{g^2 H^2 h^2}{16\pi^4} \int_{-\infty}^{\infty} dx \int_{-\infty}^{\infty} dy \ e^{-x^2 - y^2 - 2i\omega\sigma y} \left[ \operatorname{Ei} \left( -\frac{2i\tilde{\epsilon}}{H} e^{-hx} \sinh\left(h(y - i\epsilon\right)\right) \right]^2 \\
= \frac{g^2 H^2 h^2 e^{-\omega^2 \sigma^2}}{16\pi^3} \left[ \left( \gamma + \ln\frac{2\tilde{\epsilon}}{H} + \ln\left(h(\omega + \epsilon)\right) + \frac{h^2}{2} \right)^2 + \frac{h^2}{2} \right]$$
(B16)

$$-\frac{g^{2}H^{2}h^{2}}{16\pi^{4}} \int_{-\infty}^{\infty} dx \int_{-\infty}^{\infty} dy \ e^{-x^{2}-y^{2}-2i\omega\sigma y} \operatorname{Ei}\left(-\frac{2i\tilde{\epsilon}}{H}e^{-hx}\sinh\left(h(y-i\epsilon)\right)\right)$$

$$=\frac{g^{2}H^{2}h^{2}e^{-\omega^{2}\sigma^{2}}}{16\pi^{3}} \left(\gamma + \ln\frac{2\tilde{\epsilon}}{H} + \ln\left(h(\omega+\epsilon)\right) + \frac{h^{2}}{2}\right)$$
(B17)

$$\frac{g^{2}H^{2}h^{2}}{64\pi^{4}} \int_{-\infty}^{\infty} dx \int_{-\infty}^{\infty} dy \ e^{-x^{2}-y^{2}-2i\omega\sigma y} \frac{\operatorname{Ei}\left(-\frac{2i\tilde{\epsilon}}{H}e^{-hx}\sinh\left(h(y-i\epsilon)\right)\right)}{\left[\sinh(h(y-i\epsilon))\right]^{2}}$$

$$= \frac{g^{2}H^{2}e^{-\omega^{2}\sigma^{2}}}{64\pi^{3}\Omega^{2}} \left(\gamma + \ln\frac{2\tilde{\epsilon}}{H} + \ln\left(h(\omega + \epsilon)\right)\right) \tag{B18}$$

Combining all these terms, we now obtain

$$\begin{split} P &= \frac{H^2 g^2 h^2}{8\pi^3} \int_0^\infty dk \; e^{-k^2} k \frac{\cosh\left(\frac{k\pi}{h}(1 - 2h\omega\sigma/\pi)\right)}{\sinh\left(\frac{k\pi}{h}\right)} + \frac{g^2 H^2 h^2}{16\pi^3} e^{-\omega^2 \sigma^2} \\ &+ \frac{g^2 H^2 h^2 e^{-\omega^2 \sigma^2}}{96\pi^3} \int_0^\infty dk \; e^{-k^2} k^3 \frac{\cosh\left(\frac{k\pi}{h}(1 - 2h\omega\sigma/\pi)\right)}{\sinh\left(\frac{k\pi}{h}\right)} \\ &+ \frac{g^2 H^2 h^2 e^{-\omega^2 \sigma^2}}{16\pi^3} \left[ \left(\gamma + \ln\frac{2\tilde{\epsilon}}{H} + \ln\left(h(\omega + \epsilon)\right) + \frac{h^2}{2}\right)^2 + \frac{h^2}{2} \right] \\ &+ \frac{g^2 H^2 h^2 e^{-\omega^2 \sigma^2}}{16\pi^3} \left(\gamma + \ln\frac{2\tilde{\epsilon}}{H} + \ln\left(h(\omega + \epsilon)\right) + \frac{h^2}{2}\right) + \frac{g^2 H^2 e^{-\omega^2 \sigma^2}}{64\pi^3 \Omega^2} \left(\gamma + \ln\frac{2\tilde{\epsilon}}{H} + \ln\left(h(\omega + \epsilon)\right)\right) \end{split}$$
(B19)

Afterwards, it can be solved numerically. Next, to compute E given by Eq. (45), we proceed similarly to the calculation of P. We use the saddle-point approximation and the approximation

given by Eq. (B15), to obtain

$$E = -\frac{g^2 H^2 h^2 e^{-\omega^2 \sigma^2}}{16\pi^{7/2}} \int_{-\infty}^{\infty} dy \ e^{-y^2} \left[ \frac{1}{4 \left( h^2 (y - i\epsilon)^2 + e^{i2h\omega\sigma} (hr/2\sigma)^2 \right)} + 1 + \gamma + \frac{1}{2} \left( \ln \left[ \frac{i\tilde{\epsilon}}{H} (-Hr + 2e^{-ih\omega\sigma} h(y - i\epsilon)) \right] + \ln \left[ \frac{i\tilde{\epsilon}}{H} (Hr + 2e^{-ih\omega\sigma} h(y - i\epsilon)) \right] \right) \right], \tag{B20}$$

which we have computed numerically.

- [1] A. Einstein, B. Podolsky and N. Rosen, Can Quantum-Mechanical Description of Physical Reality Be Considered Complete, Phys. Rev. 777 (1935).
- [2] S. Bell, On the Einstein-Podolsky-Rosen paradox, Physics 1 195 (1964).
- [3] J. F. Clauser, M. A. Horne, A. Shimony and R. A. Holt, *Proposed experiment to test local hidden-variable theories*, Phys. Rev. Lett. **23** 880 (1969).
- [4] R. F. Werner, Quantum states with Einstein-Podolsky-Rosen correlations admitting a hidden-variable model, Phys. Rev. A40, 4277 (1989).
- [5] M. A. Nielsen and I. L. Chuang (2010), Quantum Computation And Information Theory (Cambridge university press, UK).
- P. Horodecki, Separability criterion and inseparable mixed states with positive partial transposition,
   Phys. Lett. A232, 333 (1997) [arXiv:quant-ph/9703004 [quant-ph]].
- [7] W. Tittel, J. Brendel, H. Zbinden and N. Gisin, Violation of Bell inequalities by photons more than 10 km apart, Phys. Rev. Lett.81, 3563-3566 (1998) [arXiv:quant-ph/9806043 [quant-ph]].
- [8] D. Salart, A. Baas, C. Branciard, N. Gisin and H. Zbinden, Testing spooky action at a distance, Nature 454, 861-864 (2008).
- [9] M. Hotta, Quantum measurement information as a key to energy extraction from local vacuums, Phys. Rev. D78, 045006 (2008) [arXiv:0803.2272 [physics.gen-ph]].
- [10] M. Frey, K. Funo, and M. Hotta, Strong Local Passivity in Finite Quantum Systems, Phys.Rev.E 90, 012127 (2014).
- [11] I. Fuentes-Schuller and R. B. Mann, Alice falls into a black hole: Entanglement in non-inertial frames, Phys. Rev. Lett.95, 120404 (2005) [arXiv:quant-ph/0410172 [quant-ph]].
- [12] B. Reznik, Entanglement from the vacuum, Found. Phys.33, 167-176 (2003) [arXiv:quant-ph/0212044 [quant-ph]].
- [13] E. Martin-Martinez, A. R. H. Smith and D. R. Terno, Spacetime structure and vacuum entanglement, Phys. Rev. D93, no.4, 044001 (2016) [arXiv:1507.02688 [quant-ph]].
- [14] I. Fuentes, R. B. Mann, E. Martin-Martinez and S. Moradi, Entanglement of Dirac fields in an expanding spacetime, Phys. Rev. D82, 045030 (2010) [arXiv:1007.1569 [quant-ph]].

- [15] C. Anastopoulos, B. L. Hu and K. Savvidou, Quantum field theory based quantum information: Measurements and correlations, Annals Phys. 450, 169239 (2023) [arXiv:2208.03696 [quant-ph]].
- [16] H. Casini and M. Huerta, Lectures on entanglement in quantum field theory, PoSTASI2021, 002 (2023) [arXiv:2201.13310 [hep-th]].
- [17] John Preskill, Quantum information and physics: Some future directions, Journal of Modern47, no. 2-3, 127-137, (2000).
- [18] Peres, Asher, Terno and R. Daniel, Quantum information and relativity theory, Rev. Mod. Phys. 76, no. 1, 93-123, (2004).
- [19] S. P. Jordan, K. S. M. Lee and J. Preskill, Quantum Computation of Scattering in Scalar Quantum Field Theories, Quant. Inf. Comput. 14, 1014-1080 (2014) [arXiv:1112.4833 [hep-th]].
- [20] S. B. Giddings, Black holes, quantum information, and unitary evolution, Phys. Rev. D85, 124063 (2012 [arXiv:1201.1037 [hep-th]].
- [21] P. Calabrese and J. L. Cardy, Entanglement entropy and quantum field theory, J. Stat. Mech.0406, P06002 (2004) [arXiv:hep-th/0405152 [hep-th]].
- [22] S. M. Wu, H. S. Zeng and T. Liu, Quantum correlation between a qubit and a relativistic boson in an expanding spacetime, Class. Quant. Grav.39, no.13, 135016 (2022) [arXiv:2206.13733 [quant-ph]].
- [23] H. K, S. Barman and D. Kothawala, Universal role of curvature in vacuum entanglement, Phys. Rev. D109, no.6, 6 (2024) [arXiv:2311.15019 [gr-qc]].
- [24] G. Menezes, Radiative processes of two entangled atoms outside a Schwarzschild black hole, Phys. Rev. D94, no.10, 105008 (2016) [arXiv:1512.03636 [gr-qc]].
- [25] G. Menezes and N. F. Svaiter, Radiative processes of uniformly accelerated entangled atoms, Phys. Rev. A93, no.5, 052117 (2016) [arXiv:1512.02886 [hep-th]].
- [26] S. Iso, N. Oshita, R. Tatsukawa, K. Yamamoto and S. Zhang, Quantum radiation produced by the entanglement of quantum fields, Phys. Rev. D95, no.2, 023512 (2017) [arXiv:1610.08158 [hep-th]].
- [27] F. Lindel, A. Herter, V. Gebhart, J. Faist and S. Y. Buhmann, Entanglement Harvesting from Electromagnetic Quantum Fields, [arXiv:2311.04642 [quant-ph]].
- [28] C. Lima, E. Patterson, E. Tjoa and R. B. Mann, Unruh phenomena and thermalization for qudit detectors, Phys. Rev. D108, no.10, 105020 (2023) [arXiv:2309.04598 [quant-ph]].
- [29] S. Elghaayda and M. Mansour, Entropy disorder and quantum correlations in two Unruh-deWitt detectors uniformly accelerating and interacting with a massless scalar field, Phys. Scripta98, no.9, 095254 (2023).
- [30] D. Barman, S. Barman and B. R. Majhi, Entanglement harvesting between two inertial Unruh-DeWitt detectors from nonvacuum quantum fluctuations, Phys. Rev. D106, no.4, 045005 (2022) [arXiv:2205.08505 [gr-qc]].
- [31] S. Bhattacharya, S. Chakrabortty, H. Hoshino and S. Kaushal, *Background magnetic field and quantum correlations in the Schwinger effect*, Phys. Lett. B811, 135875 (2020) [arXiv:2005.12866 [hep-th]].
- [32] S. Kaushal, Fermionic entanglement in the presence of background electric and magnetic fields,

- [arXiv:2408.15309 [hep-th]].
- [33] S. Kaushal, Schwinger effect and a uniformly accelerated observer, Eur. Phys. J. C82, no.10, 872 (2022) [arXiv:2201.03906 [hep-th]].
- [34] W. G. Unruh, Notes on black-hole evaporation, Phys. Rev. D14, 870 (1976).
- [35] N. D. Birrell and P. C. W. Davies, Quantum Fields in Curved Space, Cambridge Univ. Press (1982).
- [36] F. Benatti and R. Floreanini, Entanglement generation in uniformly accelerating atoms: Reexamination of the Unruh effect, Phys. Rev. A70, no.1, 012112 (2004) [arXiv:quant-ph/0403157 [quant-ph]].
- [37] G. Salton, R. B. Mann and N. C. Menicucci, Acceleration-assisted entanglement harvesting and rangefinding, New J. Phys. 17, no.3, 035001 (2015) [arXiv:1408.1395 [quant-ph]].
- [38] J. I. Koga, G. Kimura and K. Maeda, Quantum teleportation in vacuum using only Unruh-DeWitt detectors, Phys. Rev. A97, no.6, 062338 (2018) [arXiv:1804.01183 [gr-qc]].
- [39] J. I. Koga, K. Maeda and G. Kimura, Entanglement extracted from vacuum into accelerated Unruh-DeWitt detectors and energy conservation, Phys. Rev. D100, no.6, 065013 (2019) [arXiv:1906.02843 [quant-ph]].
- [40] J. Zhang and H. Yu, Entanglement harvesting for Unruh-DeWitt detectors in circular motion, Phys. Rev. D102, no.6, 065013 (2020) [arXiv:2008.07980 [quant-ph]].
- [41] L. J. Henderson, R. A. Hennigar, R. B. Mann, A. R. H. Smith and J. Zhang, Harvesting Entanglement from the Black Hole Vacuum, Class. Quant. Grav.35, no.21, 21LT02 (2018) [arXiv:1712.10018 [quantph]].
- [42] D. Wu, S. C. Tang and Y. Shi, Birth and death of entanglement between two accelerating Unruh-DeWitt detectors coupled with a scalar field, JHEP12, 037 (2023)[arXiv:2304.12126 [gr-qc]].
- [43] E. Martin-Martinez and N. C. Menicucci, Cosmological quantum entanglement, Class. Quant. Grav.29, 224003 (2012) [arXiv:1204.4918 [gr-qc]].
- [44] E. Tjoa and R. B. Mann, Unruh-DeWitt detector in dimensionally-reduced static spherically symmetric spacetimes, JHEP03, 014 (2022) [arXiv:2202.04084 [gr-qc]].
- [45] D. Bhattacharya, K. Gallock-Yoshimura, L. J. Henderson and R. B. Mann, Extraction of entanglement from quantum fields with entangled particle detectors, Phys. Rev. D107, no.10, 105008 (2023) [arXiv:2212.12803 [quant-ph]].
- [46] A. Dhanuka and K. Lochan, Unruh DeWitt probe of late time revival of quantum correlations in Friedmann spacetimes, Phys. Rev. D106, no.12, 125006 (2022) [arXiv:2210.11186 [gr-qc]].
- [47] H. Maeso-García, J. Polo-Gómez and E. Martín-Martínez, How measuring a quantum field affects entanglement harvesting, Phys. Rev. D107, no.4, 045011 (2023) [arXiv:2210.05692 [quant-ph]].
- [48] E. Martin-Martinez and B. C. Sanders, *Precise space-time positioning for entanglement harvesting*, New J. Phys. **18**, 043031 (2016) [arXiv:1508.01209 [quant-ph]].
- [49] D. Mendez-Avalos, L. J. Henderson, K. Gallock-Yoshimura and R. B. Mann, *Entanglement harvesting of three Unruh-DeWitt detectors*, Gen. Rel. Grav. 54, no. 8, 87 (2022) [arXiv:2206.11902 [quant-ph]].
- [50] T. R. Perche, B. Ragula and E. Martín-Martínez, Harvesting entanglement from the gravitational

- vacuum, Phys. Rev. D108, no.8, 085025 (2023) [arXiv:2210.14921 [quant-ph]].
- [51] E. G. Brown, Thermal amplification of field-correlation harvesting, Phys. Rev. A88, no.6, 062336 (2013) [arXiv:1309.1425 [quant-ph]].
- [52] S. Barman, D. Barman and B. R. Majhi, Entanglement harvesting from conformal vacuums between two Unruh-DeWitt detectors moving along null paths, JHEP09, 106 (2022) [arXiv:2112.01308 [gr-qc]].
- [53] L. J. Henderson, S. Y. Ding and R. B. Mann, Entanglement harvesting with a twist, AVS Quantum Sci.4, no.1, 014402 (2022) [arXiv:2201.11130 [quant-ph]].
- [54] T. Prokopec, Gravitational wave signals in an Unruh–DeWitt detector, Class. Quant. Grav.40, no.3, 035007 (2023) [arXiv:2206.10136 [gr-qc]].
- [55] Q. Xu, S. A. Ahmad and A. R. H. Smith, Gravitational waves affect vacuum entanglement, Phys. Rev. D102, no.6, 065019 (2020) [arXiv:2006.11301 [quant-ph]].
- [56] S. Barman, I. Chakraborty and S. Mukherjee, Entanglement harvesting for different gravitational wave burst profiles with and without memory, JHEP09, 180 (2023) [arXiv:2305.17735 [gr-qc]].
- [57] Y. Nambu, Entanglement Structure in Expanding Universes, Entropy15, 1847-1874 (2013) [arXiv:1305.4193 [gr-qc]].
- [58] S. Kukita and Y. Nambu, Harvesting large scale entanglement in de Sitter space with multiple detectors, Entropy 19, 449 (2017) [arXiv:1708.01359 [gr-qc]].
- [59] M. P. G. Robbins, L. J. Henderson and R. B. Mann, Entanglement amplification from rotating black holes, Class. Quant. Grav.39, no.2, 02LT01 (2022) [arXiv:2010.14517 [hep-th]].
- [60] W. Cong, C. Qian, M. R. R. Good and R. B. Mann, Effects of Horizons on Entanglement Harvesting, JHEP10, 067 (2020) [arXiv:2006.01720 [gr-qc]].
- [61] K. Gallock-Yoshimura, E. Tjoa and R. B. Mann, Harvesting entanglement with detectors freely falling into a black hole, Phys. Rev. D104, no.2, 025001 (2021) [arXiv:2102.09573 [quant-ph]].
- [62] M. Cliche and A. Kempf, Vacuum entanglement enhancement by a weak gravitational field, Phys. Rev. D83, 045019 (2011) [arXiv:1008.4926 [quant-ph]].
- [63] A. Pozas-Kerstjens and E. Martin-Martinez, *Harvesting correlations from the quantum vacuum*, Phys. Rev. D**92**, no.6, 064042 (2015) [arXiv:1506.03081 [quant-ph]].
- [64] P. Chowdhury and B. R. Majhi, Fate of entanglement between two Unruh-DeWitt detectors due to their motion and background temperature, JHEP05, 025 (2022) [arXiv:2110.11260 [hep-th]].
- [65] D. Barman, A. Choudhury, B. Kad and B. R. Majhi, Spontaneous entanglement leakage of two static entangled Unruh-DeWitt detectors, Phys. Rev. D107, no.4, 045001 (2023) [arXiv:2211.00383 [quantph]].
- [66] D. Makarov, Quantum entanglement of a harmonic oscillator with an electromagnetic field, Sci. Rep.8, no.1, 8204 (2018).
- [67] E. G. Brown, E. Martin-Martinez, N. C. Menicucci and R. B. Mann, Detectors for probing relativistic quantum physics beyond perturbation theory, Phys. Rev. D87, 084062 (2013) [arXiv:1212.1973 [quantph]].

- [68] D. Boyanovsky, Imprint of entanglement entropy in the power spectrum of inflationary fluctuations, Phys. Rev. D98, no.2, 023515 (2018) [arXiv:1804.07967[astro-ph.CO]].
- [69] D. Rauch, J. Handsteiner, A. Hochrainer, J. Gallicchio, A. S. Friedman, C. Leung, B. Liu, L. Bulla, S. Ecker and F. Steinlechner, et al. Cosmic Bell Test Using Random Measurement Settings from High-Redshift Quasars, Phys. Rev. Lett.121, no.8, 080403 (2018) [arXiv:1808.05966[quant-ph]].
- [70] M. J. P. Morse, Statistical Bounds on CMB Bell Violation, [arXiv:2003.13562 [astro-ph.CO]].
- [71] S. Bhattacharya, S. Chakrabortty and S. Goyal, *Dirac fermion, cosmological event horizons and quantum entanglement*, Phys. Rev. D**101**, no.8, 085016 (2020) [arXiv:1912.12272 [hep-th]].
- [72] S. Bhattacharya, H. Gaur and N. Joshi, Some measures for fermionic entanglement in the cosmological de Sitter spacetime, Phys. Rev. D102, no.4, 045017 (2020) [arXiv:2006.14212 [hep-th]].
- [73] M. S. Ali, S. Bhattacharya, S. Chakrabortty and S. Kaushal, Fermionic Bell violation in the presence of background electromagnetic fields in the cosmological de Sitter spacetime, Phys. Rev. D104, no.12, 125012 (2021) [arXiv:2102.11745 [hep-th]].
- [74] J. Foo, S. Onoe, R. B. Mann and M. Zych, Thermality, causality, and the quantum-controlled Unruh-de Witt detector, Phys. Rev. Res. 3, no. 4, 043056 (2021) [arXiv:2005.03914 [quant-ph]].
- [75] G. L. Ver Steeg and N. C. Menicucci, Entangling power of an expanding universe, Phys. Rev. D79, 044027 (2009) [arXiv:0711.3066 [quant-ph]].
- [76] S. Brahma, J. Calderón-Figueroa, M. Hassan and X. Mi, Momentum-space entanglement entropy in de Sitter spacetime, Phys. Rev. D108, no.4, 043522 (2023) [arXiv:2302.13894 [hep-th]].
- [77] S. Brahma and A. N. Seenivasan, Probing the curvature of the cosmos from quantum entanglement due to gravity, [arXiv:2311.05483 [gr-qc]].
- [78] A. Bhattacharyya, S. Brahma, S. S. Haque, J. S. Lund and A. Paul, *The Early Universe as an Open Quantum System: Complexity and Decoherence*, [arXiv:2401.12134 [hep-th]].
- [79] R. Bousso, A. Maloney and A. Strominger, Conformal vacua and entropy in de Sitter space, Phys. Rev. D65, 104039 (2002) [arXiv:hep-th/0112218 [hep-th]].
- [80] B. Garbrecht and T. Prokopec, Unruh response functions for scalar fields in de Sitter space, Class. Quant. Grav.21, 4993-5004 (2004) [arXiv:gr-qc/0404058 [gr-qc]].
- [81] M. S. Ali, S. Bhattacharya and K. Lochan, Unruh-DeWitt detector responses for complex scalar fields in de Sitter spacetime, JHEP03, 220 (2021) [arXiv:2003.11046 [hep-th]].
- [82] B. Allen, Vacuum States in de Sitter Space, Phys. Rev. D32, 3136 (1985).
- [83] J. Louko and V. Toussaint, *Unruh-DeWitt detector's response to fermions in flat spacetimes*, Phys. Rev. D**94**, no. 6, 064027 (2016) [arXiv:1608.01002 [gr-qc]].
- [84] I. S. Gradshteyn and I. M. Ryzhik, Table of integrals, series, and products, Academic Press, NY (1965).
- [85] S. Y. Lin, Unruh-DeWitt-type monopole detector in (3+1)-dimensional space-time, Phys. Rev. D68, 104019, (2003).
- [86] D. E. Bruschi, A. R. Lee and I. Fuentes, Time evolution techniques for detectors in relativistic quantum information, J. Phys. A46, 165303 (2013) [arXiv:1212.2110 [quant-ph]].

- [87] L. Sriramkumar and T. Padmanabhan, Response of finite time particle detectors in noninertial frames and curved space-time, Class. Quant. Grav.13, 2061-2079 (1996) [arXiv:gr-qc/9408037 [gr-qc]].
- [88] G. Vidal and R. F. Werner, Computable measure of entanglement, Phys. Rev. A65, 032314 (2002) [arXiv:quant-ph/0102117].
- [89] M. B. Plenio, Logarithmic negativity: a full entanglement monotone that is not convex, Phys. Rev. Lett. 95, 090503 (2005).
- [90] P. Calabrese, J. Cardy and E. Tonni, Entanglement negativity in extended systems: A field theoretical approach J. Stat. Mech. 1302, P02008 (2013) [arXiv:1210.5359 [cond-mat.stat-mech]].
- [91] S. P. Miao, N. C. Tsamis and R. P. Woodard, De Sitter Breaking through Infrared Divergences, J. Math. Phys. 51, 072503 (2010) [arXiv:1002.4037 [gr-qc]].
- [92] M. Zych, F. Costa, J. Kofler and C. Brukner, Entanglement between smeared field operators in the Klein-Gordon vacuum, Phys. Rev. D 81, 125019 (2010) [arXiv:1003.3354 [quant-ph]].
- [93] G. Kaplanek and C. P. Burgess, Hot Cosmic Qubits: Late-Time de Sitter Evolution and Critical Slowing Down, JHEP02, 053 (2020) [arXiv:1912.12955 [hep-th]].
- [94] C. P. Burgess, T. Colas, R. Holman, G. Kaplanek and V. Vennin, Cosmic Purity Lost: Perturbative and Resummed Late-Time Inflationary Decoherence, [arXiv:2403.12240 [gr-qc]].